18th Brazilian Congress of Thermal Sciences and Engineering
November 16-20, 2020 (Online)

ENC-2020-0204
SATURATION BOILING OF HFE-7100 ON COPPER SURFACES: BUBBLE DEPARTURE DIAMETER AND BUBBLE FREQUENCY

Isabela Ignácio da Silva[1], isabela.ignacio@unesp.br
Bruno Alves de Andrade[1], bruno.a.andrade@unesp.br
[1]UNESP – São Paulo State University, Post-Graduation Program in Mechanical Engineering, Av. Brasil, 56, 15385-000, Ilha Solteira, SP, Brazil.

Leonardo Lachi Manetti[1], leonardo.manetti@unesp.br
[1]UNESP – São Paulo State University, Post-Graduation Program in Mechanical Engineering, Av. Brasil, 56, 15385-000, Ilha Solteira, SP, Brazil

Jeferson Diehl de Oliveira[2], jeferson.oliveira@fsg.edu.com
[2]Centro Universitário da Serra Gaúcha, Campus Sede, Av. Rua Os Dezoito do Forte, 2366, 95020-472, Caxias do Sul, RS, Brasil

Elaine Maria Cardoso[1,3], elaine.cardoso@unesp.br
[1]UNESP – São Paulo State University, Post-Graduation Program in Mechanical Engineering, Av. Brasil, 56, 15385-000, Ilha Solteira, SP, Brazil
[3]UNESP - São Paulo State University, Campus of São João da Boa Vista, São João da Boa Vista, SP, Brazil

Abstract. *The growing demand for techniques that optimize the heat transfer process, especially those involving phase change, makes it necessary to understand the dynamics of the vapor bubble in the boiling process. Thus, this study aims to analyze the bubble dynamics for pool boiling of HFE-7100 (at saturated conditions) on a plain copper surface. Experimental tests were performed and recorded to visualize the bubble dynamics. The analysis of the vapor bubble departure diameter and vapor bubble frequency was done by using a tracking method software. The results obtained were compared with those present in the literature. We found that the experimental data are in agreement with the theoretical models of Fritz (1935) and Phan et al. (2010) for the bubble departure diameter, and Zuber (1963) and Jakob and Fritz (1931) for the bubble frequency.*

Keywords: *bubble departure diameter, bubble frequency, heating surface, pool boiling.*

1. INTRODUCTION

The increasing evolution of electronic components and their consequent miniaturization (nanotechnology) requires thermal systems capable of dissipating large amounts of heat safely (Leong et al., 2017). The pool boiling can be considered one of the most effective ways to obtain a great amount of heat exchange, with a high heat transfer coefficient (HTC) and easy to implement as compared to other existing systems - it does not use forced convection methods (Thiagarajan et al., 2015).

The understanding of the mechanisms of nucleation and vapor bubble departure is fundamental for the optimization of thermal systems involving phase change phenomena. Several authors have dedicated their studies to obtain models for the bubble departure diameter (D_d) and bubble frequency (f). Fritz (1935) was the pioneer in modeling the bubble departure diameter (D_d), considering the principle of static equilibrium of the forces acting on the vapor bubble during the boiling process. Based on Fritz's model (1935), other authors modified it and obtained new models, such as Cole and Rohsenow (1968) who introduced Jacob's number and a constant C to replace the contact angle. Some studies such as by Hamzekhani et al. (2014) and Thiagaranjam et al. (2015) used experimental data to obtain a correlation for the bubble departure diameter (D_d). Authors such as Jakob and Fritz (1935), Zuber (1963), and Mikic and Rohsenow (1969) obtained correlations for the bubble frequency (f) taking into account the thermophysical properties of the fluid, the contact angle, and the cavity size. Table 1 and Table 2 show some correlations for the vapor bubble departure diameter (D_d) and vapor bubble frequency (f), respectively.

Table 1. Models and correlations for the vapor bubble departure diameter.

Authors	Models/Correlations
Fritz (1935)	$D_d = 0.0208\theta \left(\frac{\sigma}{g\Delta\rho}\right)^{0,5}$
Borinshansky and Fokin (1963)	$D_d = 5.0 \times 10^5 \left(\frac{P}{P_c}\right)^{-0,46}$
Cole and Rohsenow (1968)	$D_d = CJa^{\frac{5}{4}}\left(\frac{\sigma}{g\Delta\rho}\right)^{0,5}$
Kocamustafaogullari (1983)	$D_d = 2.64 \times 10^{-5}\left(\frac{\sigma}{g\Delta\rho}\right)^{0,5}\left(\frac{\Delta\rho}{\rho_l}\right)$
Stephan (1992)	$D_d = 0.25\left[1 + \left(\frac{Ja}{Pr}\right)^2 \frac{100000}{Ar}\right]^{\frac{1}{2}}\left(\frac{2\sigma}{g\Delta\rho}\right)^{0,5}$
Lee et al (2003)	$D_d = \left(50\alpha\sqrt{27}\,Ja\sqrt{\frac{\rho_l}{\sigma}}\right)^2$
Kim and Kim (2006)	$D_d = 0.1649\left(\frac{\sigma}{g\Delta\rho}\right)^{0,5} Ja^{0,7}$
Phan et al. (2010)	$D_d = \left(6\sqrt{3/2}\right)^{\frac{1}{3}}\left(\frac{\rho_l}{\rho_v}\right)^{\frac{-1}{2}}\left(\frac{\rho_l}{\rho_v} - 1\right)^{\frac{1}{3}} \tan\theta^{\frac{-1}{6}} L_c$
Nam et al. (2011)	$D_d = \sqrt{24(sin\theta)^2/(2 + 3cos\theta - (cos\theta)^3)}\left[\frac{\sigma}{g\Delta\rho}\right]^{1/2}$
Hamzenkhani et al. (2014)	$D_d = \sqrt{\left(\frac{\sigma}{g\Delta\rho}\right)\left(\frac{\mu_v v_b}{\sigma cos\theta}\right)^{0,25}\left(\frac{\rho_l C_{pl}\Delta T}{\rho_v h_{lv}}\right)^{0,775}\left[\frac{g\rho_l\Delta\rho}{\mu_l{}^2}\left(\frac{\sigma}{g\Delta\rho}\right)^{1,5}\right]^{0,05}}$

Table 2. Correlations and models for the vapor bubble frequency.

Authors	Models/Correlations
Jakob and Fritz (1935)	$fD_d = 0.078$
Peebles and Garber (1953)	$fD_d = 1.18\left[\frac{t_g}{t_g + t_w}\right]\left[\frac{\sigma g\Delta\rho}{\rho_l{}^2}\right]^{\frac{1}{4}}$
McFadden and Grassman (1962)	$fD_d^{0,5} = 1.75$
Zuber (1963)	$fD_d = \left(\frac{1.18}{2}\right)\left[\frac{\sigma g\Delta\rho}{\rho_l{}^2}\right]^{\frac{1}{4}}$
Mikic and Rohsenow (1969)	$f^{\frac{1}{2}}D_d = \left(\frac{4}{\pi}\right)Ja\sqrt{3\pi\alpha_l}\left[\left(\frac{t_g}{t_g + t_w}\right)^{\frac{1}{2}} + \left(1 + \frac{t_g}{t_g + t_w}\right)^{\frac{1}{2}} - 1\right]$
Malenkov (1971)	$fD_d = \frac{V_b}{\pi}\left(1 - \frac{q}{V_b\rho_v h_{lv}}\right)$

Stephan (1992)	$fD_d = \frac{1}{\pi}\left[\frac{g}{2}\left(D_d - \frac{4\sigma}{\rho_l g D_d}\right)\right]^{\frac{1}{2}}$
Kumada and Sakashita (1995)	$f = \frac{0.215\left[\frac{g(\rho_l - \rho_v)}{\rho_l}\right]^{\frac{5}{9}}}{(v_l D_s^3)^{\frac{1}{9}}}$
Sakashita and Oho (2009)	$f = 0.6\left[\frac{g\Delta\rho}{\rho_l}\right]^{\frac{2}{3}}\left\{v_l\left[\frac{g\Delta\rho\rho_l{}^2 v_l{}^4}{\sigma^3}\right]^{-0,25}\right\}^{\frac{-1}{3}}$
Hamzekhani et al. (2015)	$f = 0.015\left(\frac{g^{0,75}\Delta\rho^{0,25}}{\sigma^{0,25}}\right)\left(\frac{q}{g^{0,75}\Delta\rho^{0,25}\sigma^{0,75}}\right)^{0,44}\left(\frac{g^{0,75}\Delta\rho^{0,25}D_d}{\sigma^{0,5}}\right)^{0,88}$

One may observe that many correlations focus on the physics of boiling phenomenon predicting the vapor bubble departure diameter and frequency. However, its usefulness decreases very quickly when the parameters deviate from the range for which the correlation was developed. Thus, it is important to carry out an analysis that improves the understanding of the fundamental mechanisms of pool boiling. In this work, we aim to find the model and/or correlation that better fits our experimental data using HFE-7100 at saturated conditions, as the working fluid.

2. METHODOLOGY

2.1 Experimental bench

The experimental apparatus for the pool boiling tests consisted of a boiling chamber, as shown in Figure 1, connected to other equipment (thermocouples, a pressure transducer, and a thermostatic bath) to perform the data acquisition. The heating surface used in the experiments consisted of a plain copper surface, with dimensions of 16 x 16 mm^2 and 60mm height, polished with sandpaper #600 (corresponds to average surface roughness, R_a = 0.14 μm). The working fluid used was HFE-7100 at saturated conditions (at local atmospheric pressure, p_{atm}= 98 kPa). Three K-type thermocouples were fixed in the copper block to estimate the wall temperature and the heat flux ($q''_{measured}$). The thermal insulation of the test section consists of polytetrafluoroethylene (PTFE). The pressure uncertainty given by Omega® was ± 0.05 kPa. The experimental uncertainties were calculated by using the method described by Moffat (1988), where the differential uncertainty of the K-type thermocouples was ± 0.3 °C (after the calibration); the heat flux and the heat transfer coefficient varied from 18.3 to 3.3 % and from 18.4 to 3.8 %, respectively (the experimental uncertainties are higher for low heat fluxes, decreasing as heat fluxes increase).

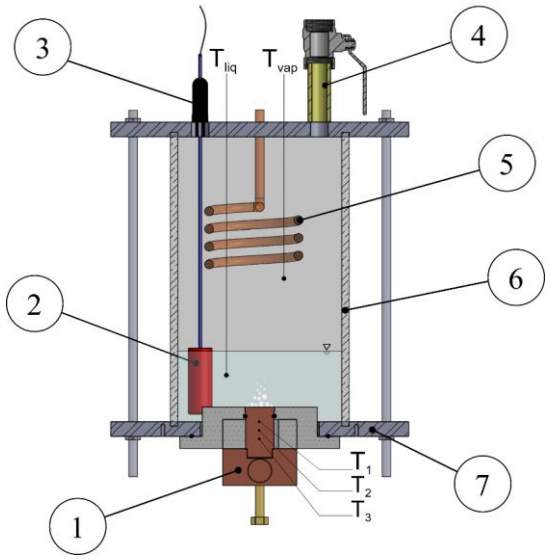

1. Test section
2. Auxiliary heater
3. Pressure transducer
4. Feed valve
5. Condenser
6. Glass chamber
7. Stainless steel plate.

Figure 1. Schematic drawing of the experimental apparatus for the pool boiling tests.

In order to study the vapor bubble dynamics, a 1000 frames per second high-speed camera (Photron FASTCAM SA3) was used, with a maximum picture resolution of 1024 × 1024 pixels (Figure 2). The test conditions were adjusted by monitoring the pressure and the temperature inside the boiling chamber. Only the temperature data for the last 500 s of the test interval were considered to ensure the steady-state regime was achieved.

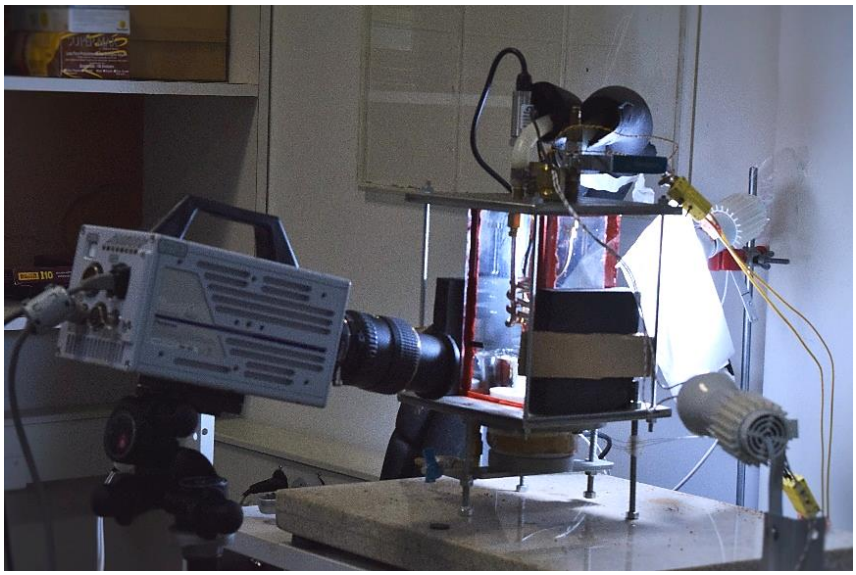

Figure 2. High-speed camera used during the pool boiling tests.

2.2 Processing of images

Through videos and image tracking software (Tracker®), the bubble departure diameter (D_d) was calculated by averaging three diameter measurements immediately after the instant that the bubble detached from the surface, as explained by Thiagarajan et al. (2015); for each heat flux, the diameters were measured at least for three different sites during a 1-second recording. Then, the arithmetic average diameters of all the evaluated bubbles for a certain experimental condition were calculated.

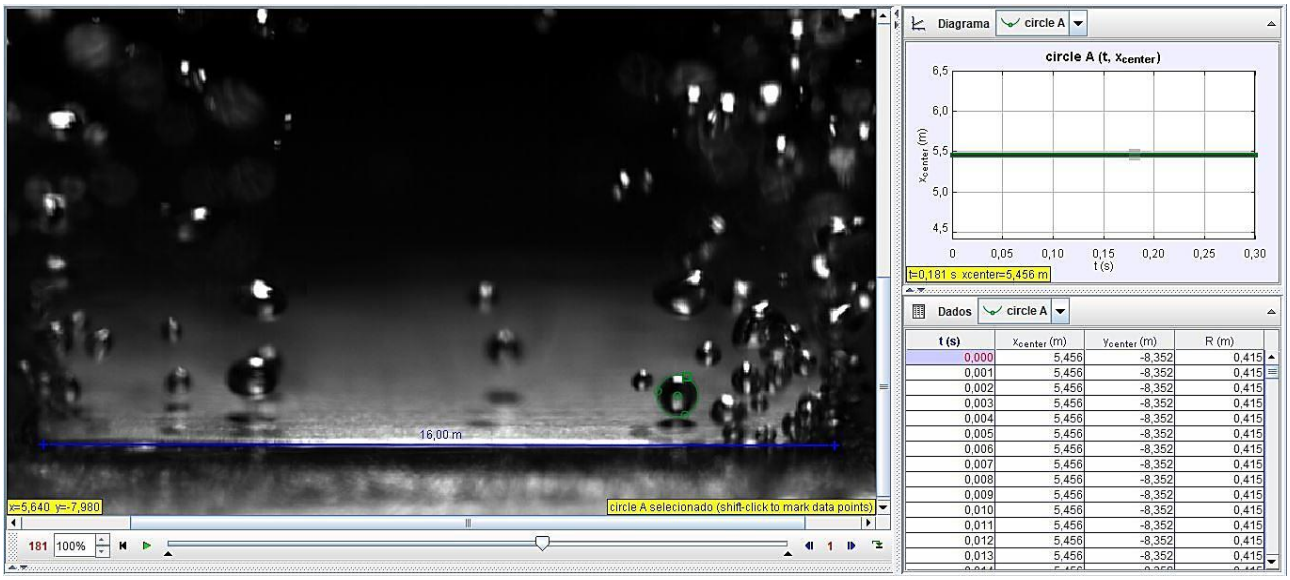

Figure 3. Measurement of characteristics of vapor bubbles.

A function called *Circle fitter* was capable of measuring the vapor bubble diameter; by selecting three points capable of forming a circle around the vapor bubble, the function returned the values of the vapor bubble radius. As the frames were changed to the next thousandth second, it was possible to change the circle to the new bubble size, making the measurement track its real dimension. Therefore, the vapor bubble diameter was measured immediately after the bubble detached from the heating surface.

As the heat flux increases, the coalescence of the vapor bubbles makes measurements above 30 kW/m² difficult and not reliable; therefore, measurements of vapor bubble departure diameter and bubble frequency were performed only for low heat fluxes (< 30 kW/m^2).

3. RESULTS

Table 3 shows the bubbles images for pool boiling tests with HFE-7100, at saturated conditions, on the plain copper surface. The heat flux applied were 23 kW/m^2, 25 kW/m^{2,} and 35 kW/m^2.

Table 3. Vapor bubbles visualization at low heat flux for the plain copper surface.

$q''_{applied}\ (kW/m^2)$	23	25	35
$q''_{measured}\ (kW/m^2)$	14.6	17.3	26.2
$\Delta T\ (K)$	14.4	15.0	16.3
Image sample	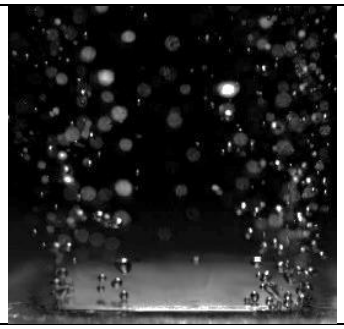		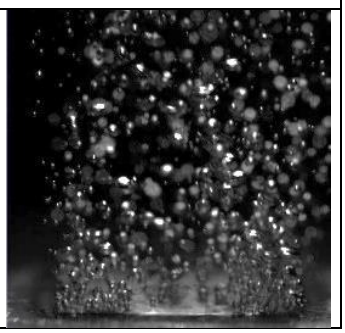

One may observe that by increasing the heat flux applied, the rate of vapor bubble formation is intensified; but, there is still a gap between the bubbles and the natural convection predominates as the heat transfer mechanism (the wall superheating slightly increases, affecting negatively the heat transfer performance).

3.1 Bubble dynamics

Through videos and image tracking software, it was possible to compare the results obtained experimentally for the bubble departure diameter and bubble frequency with several theoretical models and correlations from the literature.

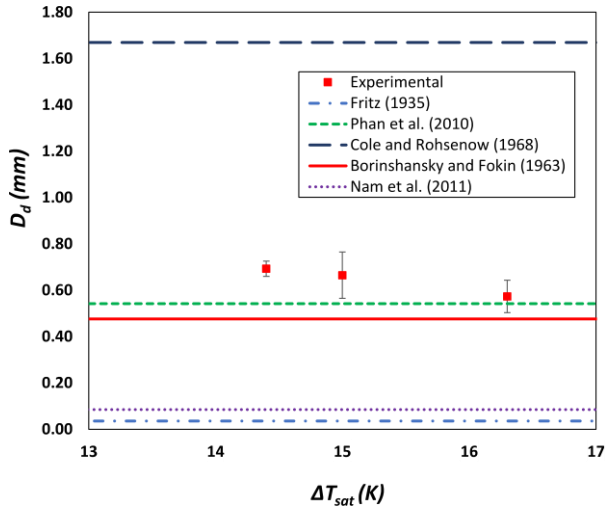

(a)

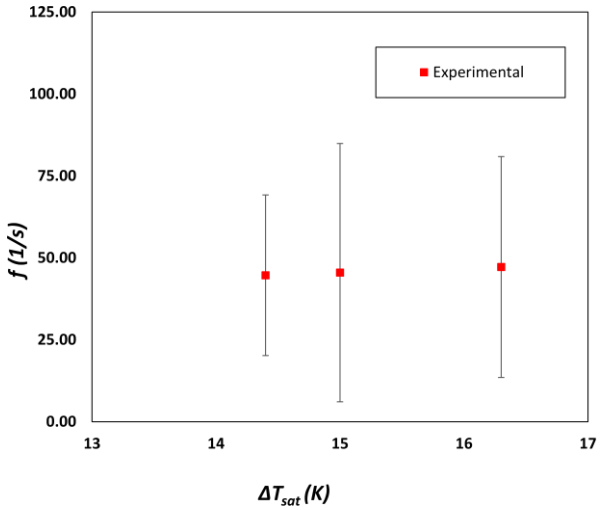

(b)

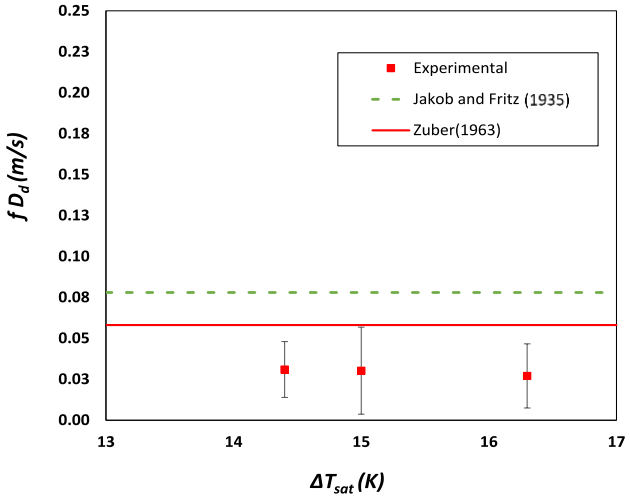

(c)

Figure 4. Bubble dynamics results: (a) comparison of experimental bubble departure diameter with models and correlations from literature; (b) experimental data for vapor bubble frequency; (c) comparison of experimental bubble frequency models and correlations from literature.

By analyzing the bubble departure diameter in Figure 4a, Fritz's model (1935) and the correlation of Nam et al. (2011) drastically underpredict the measured departure diameters due to the dependence on the contact angle. Thus, for wetting fluids - with contact angle < 10°, such as HFE-7100 - other correlations/models can better predict the experimental data; Cole and Rohsenow correlation (1968) even takes into account the thermal properties of the working fluid, over-estimated the vapor bubble diameter. The correlation of Borishanskiy and Fokin (1963) is also a function of thermal properties and includes critical pressure in his formulation, showing a reasonable agreement with the experimental data (with an average absolute deviation, AAD, of 25.5%). The correlation of Phan et al. (2010) considered the contact angle in a trigonometric equation that also incorporates the influence of fluid properties and gravity, showing that the trend predicted by the model matches well with the present data (with an AAD of 15.1%).

$$\mathrm{AAD} = \frac{\sum_{i=1}^{N} \left| \frac{\text{predicted value - experimental value}}{\text{experimental value}} \right|}{N} \times 100 \tag{1}$$

Figure 4c shows that the model of Jakob and Fritz (1935) and Zuber (1963) reasonably predicted the experimental data (showing a deviation of 53.4% and 49.2%, respectively). The former studied the bubble departure of saturated water on a roughened plain surface at atmospheric pressure and postulated the product of departure frequency (f) and diameter (D_d) to be a constant; the latter derived the correlation based on the assumption that growth time was equal to waiting time. As mentioned by Dhir (1998) and Chen et al. (2017), predictions of vapor bubble frequency based on waiting (t_w) and growth (t_g) times do not match well with experimental data because many simplifications are made in obtaining these values (t_w and t_g).

4. CONCLUSION

Based on the results obtained in this study, the methodology of measuring the bubble departure diameter (D_d) and bubble frequency (f) was validated with experimental data and models and correlations from the literature. The correlations of Borishanskiy et al. (1981) and Phan et al. (2010) presented satisfactory results and were close to the experimental data for the bubble departure diameter (D_d), showing an average absolute deviation of 25.5% and 15.1%, respectively). For the vapor bubble frequency (f), the experimental data were in agreement with Zuber (1963) and Jakob and Fritz's (1931) models.

5. ACKNOWLEDGMENTS

The authors are grateful for the financial support from PPGEM – UNESP/FEIS, CAPES, and FAPESP (grants number 2013/15431-7, 2019/13895-2, and 2019/02566-8). The authors also extend their gratitude to Anderson Giacomeli Fortes for his important contribution to this work.

NOMENCLATURE

t_w bubble waiting period [s]
t_g bubble growth period [s]
f bubble departure frequency [1/s]
g gravity [m/s^2]
D_d bubble departure diameter [m]
Ja Jakob number [-]
V_b bubble departure volume [m^3]
h_{lv} latent heat of vaporization [J/kg]
C_{pl} liquid-phase specific heat at constant pressure [J/kg ·K]
L_c capillary length $(\sigma/g\Delta\rho)^{0,5}$ [mm]
P pressure [Pa]
P_c pressure cavity [Pa]
C thermal capacity [J/K]
v_l specific volume [m^3/kg]

Greek symbols

σ surface tension [N/m]
ρ_l liquid phase density [kg/m^3]
ρ_v vapor phase density [kg/m^3]
θ contact angle [°]
$\Delta\rho$ density variation [kg/m^3]
μ_v vapor dynamic viscosity [kg/m·s]
μ_l liquid dynamic viscosity [kg/m·s]
α thermal diffusivity [m^2/s]

6. REFERENCES

Borinshansky VM, Fokin FS. Heat transfer and hydrodynamics in steam generators. Trudy TsKTI, v. 62, n. 1, 1963.

Chen H, Chen G, Zou X, Yao Y, Gong M. Experimental investigations on bubble departure diameter and frequency of methane saturated nucleate pool boiling at four different pressures. Int J Heat Mass Transf 2017; 112: 662-675.

Cole R, Rohsenow WM. Correlation of bubble departure diameters for boiling of saturated liquids. Chem Eng Prog Symp Ser 1968;65(92):211–3.

Dhir VK. Boiling Heat Transfer. Annu. Rev. Fluid Mech. 1998. 30:365–401.

Fritz W. Maximum volume of vapor bubbles. Phys Z. 1935;36:379–84.

Hamzekhani S, Falahieh MM, Akbari A. Bubble departure diameter in nucleate pool boiling at saturation: pure liquids and binary mixtures. Int J Refrig 2014;46:50–8.

Hamzekhani S, Falahieh MM, Kamalizadeh MR, Nazari Z. Experimental study on bubble departure frequency for pool boiling of water/NaCl solutions. Heat Mass Transf 2015;51:1313–20.

Jamialahmadi M, Helalizadeh A, Muller-Steinhagen H. Pool boiling heat transfer to electrolyte solutions. Int J Heat Mass Transf 2004;47:729–42.

Jakob M, Fritz W. Versuche uber den verdampfungsvorgang. Forsch auf dem Geb Des Ing 1931;2:435–47.

Kim J, Kim MH. On the departure behaviours of bubble at nucleate pool boiling. J Multiph Flow 2006;32:1269–86.

Kocamustafaogullari G. Pressure dependence of bubble departure diameter for water. Int Commun Heat Mass Transf 1983;10:501–9.

Kumada T, Sakashita H. Pool boiling heat transfer-I. measurement and semi-empirical relations of detachment frequencies of coalesced bubbles. Int J Heat Mass Transf 1995;38(6):969–77.

Lee HC, Oh BD, Bae SW, Kim HM. Single bubble growth in saturated pool boiling on a constant wall temperature surface. Int J Multiph Flow 2003;29:1857–74.

Leong KC, Ho JY, Wong KK. A critical review of pool and flow boiling heat transfer of dielectric fluids on enhanced surfaces. Appl. Therm. Eng 2017;112:999-1019.

Malenkov IG. Detachment frequency as a function of size of vapor bubbles (transl.). Inzh Fiz Zh 1971;20(2):988.

McFadden PW, Grassman P. The relation between bubble frequency and diameter during nucleation pool boiling. Int J Heat Mass Transf 1962;5:169–73.

Mikic BB, Rohsenow WM. Bubble growth rates in non-uniform temperature field. Prog Heat Mass Transf 1969;2:283–93.

Moffat RJ. Describing the uncertainties in experimental results. Exp. Therm. Fluid Sci. 1988;1 (1):3-17.

Nam Y, Aktinol E, Dhir VK, Sungtaek Ju Y. Single bubble dynamics on a superhydrophilic surface with artificial nucleation sites. Int J Heat Mass Transf 2011;54(7):1572-1577.

Peebles FN, Garber HJ. Study on motion of gas bubbles in liquids. Chem Eng Prog 1953;49:88–97

Phan HT, Caney N, Marty P, Colasson S, Gavillet J. A model to predict the effect of contact angle on the bubble departure diameter during heterogeneous boiling. Int Commun Heat Mass Transf 2010;37:964–9.

Sakashita H, Ono A. Boiling behaviours and critical heat flux on a horizontal plate in saturated pool boiling of water at high pressures. Int J Heat Mass Transf 2009;52:744–50.

Stephan K. Heat transfer in condensation and boiling. New York: Springer; 1992.

Stephan K. Saturated pool boiling and sub-cooled flow boiling of mixtures (Ph.D. thesis). New Zealand: University of Auckland; 1992.

Thiagarajan SJ, Yang R, King C, Narumanchi S. Bubble dynamics and nucleate pool boiling heat transfer on microporous copper surfaces. Int J Heat Mass Transf 2015;89:1297-1315.

Tracker®. Video Analysis and Modeling Tool. https://physlets.org/tracker/.

Zuber N. Nucleate boiling. The region of isolated bubbles and the similarity with natural convection. Int J Heat Mass Transf 1963;6:53–78.

7. RESPONSIBILITY NOTICE

The authors are the only responsible for the printed material included in this paper.